Permeation and block of rat GluR6 glutamate receptor channels by internal and external polyamines

Robert Bähring*, Derek Bowie*, Morris Benveniste† and Mark L. Mayer‡

Laboratory of Cellular and Molecular Neurophysiology, National Institute of Child Health and Human Development, NIH, Bethesda, MD 20892, USA and †Department of Physiology and Pharmacology, Sackler School of Medicine, Tel Aviv University, Israel 69978

1. Polyamine block of rat GluR6(Q) glutamate receptor channels was studied in outside-out patches from transiently transfected HEK 293 cells. With symmetrical 150 mM Na^+ and 30 μM internal spermine there was biphasic voltage dependence with 95% block at +40 mV but only 20% block at +140 mV. Dose–inhibition analysis for external spermine also revealed biphasic block; the K_d at +40 mV (54 μM) was lower than at +80 (167 μM) and −80 mV (78 μM).

2. For internal polyamines relief from block was most pronounced for spermine, weaker for *N*-(4-hydroxyphenylpropanoyl)-spermine (PPS), and virtually absent for philanthotoxin 343 (PhTX 343), suggesting that permeation of polyamines varies with cross-sectional width (spermine, 0·44 nm; PPS, 0·70 nm; PhTX 343, 0·75 nm).

3. With putrescine, spermidine, or spermine as sole external cations, inward currents at −120 mV confirmed permeation of polyamines. For bi-ionic conditions with 90 mM polyamine and 150 mM Na_i^+, reversal potentials were −12·4 mV for putrescine (permeability ratio relative to Na^+, $P_{Put}/P_{Na} = 0{\cdot}42$) and −32·7 mV for spermidine ($P_{Spd}/P_{Na} = 0{\cdot}07$). Currents carried by spermine were too small to analyse accurately in the majority of patches.

4. Increasing $[Na^+]_i$ from 44 to 330 mM had no effect on the potential for 50% block ($V_{½}$) by 30 μM internal spermine; however, relief from block at positive membrane potentials increased with $[Na^+]_i$. In contrast, raising $[Na^+]_o$ from 44 to 330 mM resulted in a depolarizing shift in $V_{½}$, indicating a strong interaction between internal polyamines and external permeant ions.

5. The Woodhull infinite barrier model of ion channel block adequately described the action of spermine at membrane potentials insufficient to produce relief from block. For 30 μM internal spermine such analysis gave $K_{d(0)} = 2{\cdot}5$ μM, $z\theta = 1{\cdot}97$; block by 30 μM external spermine was weaker and less voltage dependent ($K_{d(0)} = 37{\cdot}8$ μM and $z\delta = 0{\cdot}55$); δ and θ are electrical distances measured from the outside and inside, respectively.

6. Fits of the Woodhull equation for a permeable blocker adequately described both onset and relief from block by spermine over a wide range of membrane potentials. However, the rate constants and $z\delta$ values estimated for block by internal spermine predicted much stronger external block than was measured experimentally, and vice versa.

7. An Eyring rate theory model with two energy wells and three barriers explained qualitatively many characteristic features of the action of polyamines on GluRs, including biphasic *I–V* relationships, weaker block by external than internal spermine and low permeability.

* The authors have contributed equally to this work.

‡ To whom correspondence should be addressed at Building 49, Room 5A78, 49 Convent Drive, MSC 4495, Bethesda, MD 20892, USA.

Expression cloning of AMPA and kainate receptor genes revealed rectification properties for glutamate receptors (GluRs) reminiscent of those for inward rectifier potassium (Kir) channels (Verdoorn, Burnashev, Monyer, Seeburg & Sakmann, 1991; Doupnik, Davidson & Lester, 1995). Similar to polyamine block of Kir channels (Fakler *et al.* 1994; Ficker, Taglialatela, Wible, Henley & Brown, 1994; Lopatin, Makhina & Nichols, 1994; Fakler, Brändle, Glowatzki, Weidemann, Zenner & Ruppersberg, 1995), internal polyamines produce strong block of outward current for GluR channels (Bowie & Mayer, 1995; Donevan & Rogawski, 1995; Isa, Iino, Itazawa & Ozawa, 1995; Kamboj, Swanson & Cull-Candy, 1995; Koh, Burnashev & Jonas, 1995). The most striking difference between Kir and GluR channels is that on depolarization beyond about +50 mV, in contrast to the strong block observed for Kir channels, surprisingly large outward currents develop for GluR channels (Verdoorn *et al.* 1991; Bowie & Mayer, 1995; Donevan & Rogawski, 1995; Isa *et al.* 1995; Kamboj *et al.* 1995; Koh *et al.* 1995). Although this most probably reflects relief from block due to permeation of polyamines there has been no experimental test of this hypothesis. Compared with Kir channels other key properties of GluR channels are also much less well characterized. For example, it is not known if rectification in GluR channels is coupled to shifts in the reversal potential produced by altering the permeant ion concentration as has been shown for Kir channels (Lopatin & Nichols, 1996).

The recent identification of polyamine block in GluR channels as the mechanism most likely to underlie biphasic rectification (Bowie & Mayer, 1995; Donevan & Rogawski, 1995; Isa *et al.* 1995; Kamboj *et al.* 1995; Koh *et al.* 1995) has allowed us to analyse in detail the rectification properties of GluRs. The results of our experiments highlight both similarities and differences between GluR and Kir channels, including strong coupling of polyamine block to the flux of permeant ions in both types of channel, but uniquely for GluR channels, a surprisingly high permeability for polyamines themselves. Furthermore, we demonstrate differences in the voltage dependence of block for GluR channels by internal and external spermine, and introduce an Eyring rate theory model with two energy wells and three barriers which explains qualitatively many characteristic features of the action of polyamines on GluRs, including biphasic *I–V* relationships, weaker block by external than internal spermine, as well as a low permeability measured with polyamines as sole charge carriers.

METHODS

Cell culture and expression of recombinant glutamate receptors

HEK 293 cells (American Type Culture Collection CRL 1573) were maintained at a confluency no greater than 70–80% in minimal essential medium with Earle's salts (Gibco), 2 mM glutamine and 10% (v/v) fetal bovine serum. Twenty-four hours after plating at low density onto 35 mm Petri dishes (2×10^4 cells ml^{-1}), cells were transfected as described previously using 2 × CsCl gradient purified plasmids (Bowie & Mayer, 1995). Cultures were washed with phosphate buffered saline 12–18 h after transfection and used for electrophysiological recordings after another 24–48 h. We used a rat cDNA clone for GluR6(Q) incorporated into a cytomegalovirus expression vector (a gift from Dr P. Seeburg, University of Heidelberg, Germany). Cotransfection with the cDNA for green fluorescent protein (S65T mutation) helped to identify transfected cells during experiments.

Solutions

The standard internal solution contained (mM): NaCl, 120; NaF, 10; $CaCl_2$, 0·5; Hepes, 5; and Na_4BAPTA, 5; pH 7·2. In experiments where the current–voltage relationship was studied in the absence of internal polyamine block, we used 110 mM NaCl with 10 mM Na_2ATP to chelate spermine and spermidine (Bowie & Mayer, 1995); the program BAD (Brooks & Storey, 1992) was used to calculate complex formation with ATP and hence the free Na^+ concentration. The hydrochloride salts of spermine and spermidine were purchased from Sigma; *N*-(4-hydroxyphenylpropanoyl)-spermine from Tocris Cookson, Bristol, UK; philanthotoxin 343 (PhTX 343) trifluoroacetate from RBI (in preliminary experiments we used PhTX 343 supplied by Professor K. Nakanishi, Columbia University, New York, USA); polyamines were added to the standard internal solution as required.

Unless indicated differently, the standard external solution contained (mM): NaCl, 150; $CaCl_2$, 0·1; $MgCl_2$, 0·1; and Hepes, 5; 0·01 mg ml^{-1} Phenol Red; pH 7·3; osmolarity adjusted to 295 mosmol l^{-1} with sucrose. GluR6(Q) responses were activated by 50 μM domoic acid (Tocris Cookson) dissolved in standard external solution and applied with a stepper motor-based fast perfusion system (Vyklicky, Benveniste & Mayer, 1990). Desensitization was reduced by treating patches for ~1 min with 0·3 mg ml^{-1} Sigma Type IV concanavalin A. In experiments where $[Na^+]_o$ was varied, we used 44, 120 and 330 mM external NaCl while $[Na^+]_i$ was kept constant at 120 mM; for 44 mM Na_o^+, sucrose was added to the external solution to maintain 295 mosmol l^{-1}; for 330 mM Na_o^+ (600 mosmol l^{-1}), we confirmed in the same patch that control responses with 120 mM Na_o^+ were unaffected when sucrose was added to the external solution to increase the osmolarity to 600 mosmol l^{-1}. In experiments where $[Na^+]_i$ was varied from 44 to 330 mM, the external solution always contained 120 mM Na^+; the osmolarity of the internal solution was maintained at 290 mosmol l^{-1} for 44 mM Na_i^+; no adjustment was made for 330 mM Na_i^+.

In experiments with polyamines as the sole external charge carrier, all external Na^+ was replaced by the hydrochloride salts of putrescine, spermidine or spermine, each at a concentration of 90 mM, and the pH adjusted to 7·3 with the corresponding polyamine free base. In these experiments responses with polyamines were compared with those recorded in the same patch with 150 mM *N*-methyl-D-glucamine (NMG) as the sole external charge carrier, a monovalent ion previously shown to have low permeability for GluR6(Q) channels (Burnashev, Villarroel & Sakmann, 1996).

Recording techniques

Electrodes were pulled from thin-wall borosilicate glass (WPI, TW150F-6), coated with dental wax to reduce noise, and fire polished to a tip resistance of 2–5 MΩ. Outside-out membrane patches were voltage clamped using Axopatch 200 or Axopatch 200A amplifiers, with series resistance compensation set to 95%. Current signals were filtered at 0·5–8 kHz with an 8-pole Bessel filter, amplified as required, digitized at 60–500 μs intervals and stored on Power Macintosh 7600/132 computers using 16 bit A/D converters (ITC-16) under control of the data acquisition and

analysis program Synapse (Synergy Research Incorporated, Silver Spring, MD, USA). All experiments were conducted at room temperature.

Analysis

Corey–Pauling–Koltum (CPK) space-filling models for spermine, PPS and PhTX 343 were generated using Chem3D Pro software (CambridgeSoft Corp, Cambridge, MA, USA), rotated in three dimensions to display their minimal cross-sectional area and exported as PICT files; for PhTX 343 the butyryl side chain had to be repositioned from the MM2 minimized structure to a less favourable conformation in order to minimize the cross-sectional area. To compare the voltage dependence of block by different polyamines, domoate-activated currents acquired with voltage ramps (0·4–1·6 V s^{-1}) were leak subtracted using the average of two to three control responses and fitted with a ninth-order polynomial function to determine the reversal potential (V_{rev}); identical results were obtained over the ramp rates examined. G–V relationships were calculated from the equation $G = I/(V_m - V_{rev})$ using the program Kaleidagraph (Synergy Software, Reading, PA, USA). After masking data points around V_{rev} and positive to +20 mV, G–V relationships for internal polyamine block were fitted with an infinite barrier model widely used to describe ion channel block (Woodhull, 1973):

$$G = G_{max}\left(\frac{1}{1+[P]/K_d}\right), \quad (1)$$

where:

$$K_d = K_{d(0)}\exp(-V_m z\theta F/RT).$$

G_{max} is the domoate-activated conductance at a membrane potential sufficiently hyperpolarized to relieve internal polyamine block; [P], the internal polyamine concentration; K_d, the dissociation constant at a membrane potential V_m; $K_{d(0)}$ the dissociation constant at 0 mV; z, the valence of the polyamine; and $\theta = 1 - \delta$, where δ is the fraction of the membrane electric field, measured from the extracellular face of the membrane, which the blocker molecule experiences at its binding site; F, R and T have their usual meanings. Data from individual patches were normalized to G_{max} and pooled. The Woodhull equation described above is a special case for an impermeable blocker; although the results of such analysis are useful for comparison with other studies the model is not appropriate for a blocker with significant permeability. Thus fits were also performed using the Woodhull model for the following scheme in which a blocker, X, can reach its binding site from either face of the membrane,

$$X_{out} \underset{k_{-1}}{\overset{[X]_o k_1}{\rightleftharpoons}} \text{Blocked} \underset{[X]_i k_{-2}}{\overset{k_2}{\rightleftharpoons}} X_{in}.$$

The probability (p) that the channel is not blocked is calculated as the sum of exit rates divided by the sum of all rate constants:

$$p = \frac{k_{-1} + k_2}{[X]_o k_1 + k_2 + k_{-1} + [X]_i k_{-2}}. \quad (2)$$

The rate constants k_1, k_{-1}, k_2 and k_{-2} were calculated using equations 7a and 8a from Woodhull (1973).

To compare shifts in V_{rev} caused by varying $[Na^+]_i$ or $[Na^+]_o$ with changes in voltage dependence for block by internal spermine, G–V relationships for spermine block with different ionic conditions were fitted with a Boltzmann function of the form:

$$G = G_{max}\left(\frac{1}{1+\exp((V_m - V_{½})/k)}\right), \quad (3)$$

where G, G_{max} and V_m have the same meanings as in eqn (1); $V_{½}$ is the membrane potential for half-maximal block and k is a slope factor indicating the membrane potential change necessary to induce an e-fold change in conductance.

For experiments in which external Na^+ was substituted with NMG, putrescine or spermidine permeability ratios relative to Na^+ (P_X/P_{Na}) were calculated by summing the constant field current equations for the individual ion species in bi-ionic solutions to calculate the zero current potential as a function of P_X/P_{Na}:

$$I_X = P_X z^2\left(\frac{V_m F^2}{RT}\right)\left(\frac{[X]_i - [X]_o\exp(-zFV_m/RT)}{1-\exp(-zFV_m/RT)}\right), \quad (4)$$

where I_X is current carried by ion X at a membrane potential V_m; P_X, the corresponding permeability ($P_{Na} = 1$); $[X]_i$ and $[X]_o$, the internal and external concentrations; and z, the valence. Experimentally determined V_{rev} values were used for V_m, and since at the reversal potential $I_{Na} + I_X = 0$, we were able to obtain P_X/P_{Na}. The respective reversal potentials given in the text were corrected for liquid junction potentials measured as described by Neher (1992).

To estimate the apparent dissociation constant for block by external spermine at different holding potentials, dose–inhibition plots were fitted with a modified form of the logistic equation that allowed for the experimentally observed failure to obtain complete block at high spermine concentrations:

$$I = \left(\frac{I_{max} - I_{min}}{1+[Spm]_o/K_d}\right) + I_{min}, \quad (5)$$

where I_{max} is the current amplitude measured in the absence of external spermine; I_{min}, the current amplitude in the presence of a saturating concentration of external spermine; and $[Spm]_o$, the external spermine concentration.

All data are presented as means ± S.E.M. unless otherwise stated. Statistical tests were performed using variance analysis with the program GraphPad InStat (GraphPad Software).

Modelling permeation and block using Eyring rate theory

A Macintosh program was written by M.B. to simulate and fit Eyring rate theory models for single file multi-ion pores using principles described by Begenisich & Cahalan (1980). For simplicity Na^+ and spermine were assumed to bind at the same sites, but with different energy values. For a channel with w binding sites and m ionic species the number of states (n) was calculated as:

$$n = (m+1)^w. \quad (6)$$

The rate constants for transitions between states were calculated as functions of the energy levels of the barriers and wells separating individual states for each ionic species, using absolute reaction rate theory. A matrix, $\boldsymbol{Q}$, of rate constants q_{ij}, where the row index i defines the initial state and the column j defines the final state for a given transition, was used to calculate the equilibrium occupancies of all n states as described previously (Begenisich & Cahalan, 1980; Colquhoun & Hawkes, 1987; Davies, McKillen, Stanfield & Standen, 1996).

At any given membrane potential V_m, values for q_{ij} were calculated as:

$$q_{ij} = rq'_{ij}\exp(-\delta z_b FV_m/RT), \quad (7)$$

where r is an ionic repulsion factor, defined below; q'_{ij}, the chemical component of the free energy change; δ, the electrical distance between the apex of an energy barrier and the adjacent energy well from which the transition originated; z_b, the valence of the ion b; and F, R and T have their standard meanings.

The chemical energy component q'_{ij} was defined as:

$$q'_{ij} = \gamma(kT/h)\exp(-\Delta G), \quad (8)$$

where γ is the molar activity of Na^+ or spermine and was set to 1 for all transitions other than those for entry into the pore from the intracellular and extracellular solutions; ΔG is Gibb's free energy of transition (in units of RT) determined from the free energy value of the well from which the transition originated subtracted from the free energy of the barrier over which the transition takes place. The frequency of molecular vibration (kT/h) was calculated from the Boltzmann constant, k and Planck's constant, h. The activity coefficient for Na^+ was calculated according to the Debye–Hückel theory for point charge screening (Hille, 1992); the activity coefficient for spermine was assumed to be 1.

When ionic repulsion was implemented, transitions into a well, α, where an adjacent well, β, was occupied, were slowed by a factor s ($r = 1/s$). For transitions in which an ion was exiting a well, α, to enter either an unoccupied well or one of the surface solutions and the adjacent well on the opposite side, β, was occupied, the rate constant for that transition was increased by s ($r = s$). Ionic repulsion factors were set empirically using as a guide values determined by Coulomb's law for a given distance between sites.

After solving for the occupancy of each state at a given membrane potential, net ionic current was calculated by choosing one barrier and summing the individual ionic fluxes over the barrier:

$$I = e\sum_{b=1}^{k} z_b(p_{x_b}q_{x_by_b} - p_{y_b}q_{y_bx_b}), \quad (9)$$

where p and q are the state specific occupancies and rate constants, respectively, and x_b describes a state in which ion b occupies a particular well, α, when the adjacent well β is unoccupied. y_b describes a state identical in occupancy to x_b except ion b now occupies well β with the adjacent well α unoccupied. z_b is the valence of ion b and e is the elementary electronic charge ($1{\cdot}6 \times 10^{-19}$ C).

Normalized data were fitted utilizing a Davidon–Fletcher–Powell minimization algorithm (Press, Teukolsky, Vetterling & Flannery, 1992) to minimize the sum squared errors (SSEs) between a family of experimental I–V curves and a family of simulated curves. In general, experimental data was step averaged with a step size of ten points. Only δ and ΔG values were varied during fitting. Fits were constrained by assessing penalties on the SSE values if δ values or ΔG values proved to be illogical; for instance if δ values were negative or ΔG values for wells were greater than their adjacent barriers.

RESULTS

Block of GluR6(Q) channels by internal polyamines of different structure

Because polyamines are already present in the cytoplasm of all mammalian cells, it is not possible to study in isolation the action of experimentally applied polyamines using whole-cell recording. For this reason, our experiments were performed using outside-out membrane patches with polyamines applied at known concentrations to either the internal or external face of the membrane as required. Polyamine block occurs for both AMPA and kainate subtype recombinant glutamate receptor channels (Bowie & Mayer, 1995; Kamboj *et al.* 1995). Although the polyamine sensitivity of AMPA receptors assembled from GluRA is 3-fold higher than that of kainate receptors assembled from GluR6 (Bowie & Mayer, 1995), the high levels of expression routinely obtained with GluR6 greatly facilitated analysis

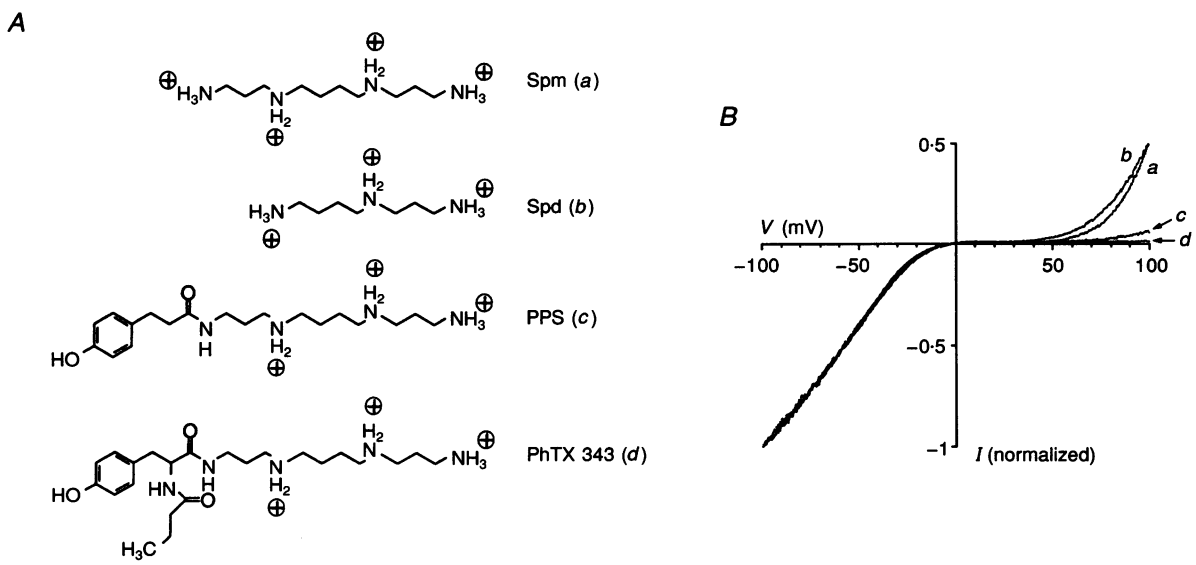

Figure 1. Current–voltage relationships for GluR6(Q) block by internal polyamines

A, structures of spermine (Spm), spermidine (Spd), *N*-(4-hydroxyphenylpropanoyl)-spermine (PPS) and philanthotoxin 343 (PhTX 343) indicating the location of positive charges generated by protonation of amino groups. *B*, I–V relationships for outside-out patch responses to 50 μM domoate during voltage ramps from −100 to +100 mV (0·4 V s^{-1}) with different polyamines in the pipette solution. Traces show pooled data from individual patches normalized to responses at −100 mV for 30 μM spermine (*a*), $n = 7$; 100 μM spermidine (*b*), $n = 4$; 100 μM PPS (*c*), $n = 5$; and 100 μM PhTX 343 (*d*), $n = 5$.

of the mechanism of rectification, and we did not study other glutamate receptor subunits in the present series of experiments.

The amine groups in spermine are separated by methylene groups with 3,4,3 spacing and when fully ionized generate a tetravalent cation with distributed charge as shown in Fig. 1*A*; at physiological pH the average charge is 3·8 (Palmer & Powell, 1974). When 30 μM spermine was included in the pipette solution, the *I–V* relationship of domoate-activated responses recorded during voltage ramps from −100 to +100 mV showed pronounced biphasic rectification, with strong relief of block depolarized to +40 mV (Fig. 1*B*). Similar results were obtained for spermidine, for which the polyamine chain is shortened by one amine and three methylene groups, generating a trivalent cation when fully ionized, with 3,4 spacing of the amine groups (Fig. 1*A*). In order to match the characteristic *I–V* recorded with 30 μM internal spermine, a spermidine concentration of 100 μM was required (Fig. 1*B*). Similar inward rectification, but without pronounced relief of block, was obtained when either of two *N*-substituted analogues of spermine were added to the internal solution. In *N*-(4-hydroxy-phenyl-propanoyl)-spermine (PPS) one terminal amine of the spermine moiety forms a peptide bond with a homotyrosine group reducing the valence to +3 (Fig. 1*A*). Similar to spermidine, the lower potency of PPS required 100 μM to produce block like that recorded with 30 μM spermine at membrane potentials from −100 to +40 mV (Fig. 1*B*); however, at more positive potentials outward currents with PPS were much smaller than with spermidine or spermine. Philanthotoxin 343 (PhTX 343), a synthetic wasp toxin analogue similar in structure to PPS, but with an additional butyryl side chain (Fig. 1*A*), was of similar potency to PPS but outward currents at positive membrane potentials were of even smaller amplitude and difficult to distinguish from the leak current (Fig. 1*B*).

Further analysis of the results shown in Fig. 1 provides strong support for the hypothesis that the biphasic *I–V* relationship observed with internal spermine and spermidine is due to permeation on depolarization above +40 mV of these relatively small diameter rod-shaped molecules. Conductance–voltage (*G–V*) relationships normalized to responses at −100 mV revealed strong block at +40 mV for 30 μM spermine, 100 μM spermidine, 100 μM PPS and 100 μM PhTX 343 (Fig. 2*A*). Fitting the Woodhull infinite barrier model for ion channel block over the range −100 to +20 mV gave $K_{d(0)}$ estimates of 2·5 ± 0·2 μM for spermine ($z\theta = 1{\cdot}97 \pm 0{\cdot}03$, $n = 12$); 13·3 ± 0·9 μM for spermidine ($z\theta = 1{\cdot}83 \pm 0{\cdot}02$, $n = 4$); 16·8 ± 3·0 μM for PPS ($z\theta = 1{\cdot}85 \pm 0{\cdot}07$, $n = 5$); and 12·7 ± 1·8 μM for PhTX 343 ($z\theta = 1{\cdot}84 \pm 0{\cdot}08$, $n = 5$). Adding 1 mM Mg^{2+} to the internal solution did not produce voltage dependent block and also did not interfere with block by 30 μM spermine ($K_{d(0)} = 3{\cdot}1 \pm 1{\cdot}2$ μM, $z\theta = 1{\cdot}86 \pm 0{\cdot}11$, $n = 3$). Although block by 30 μM internal spermine reached a maximum of 96 ± 0·5% ($n = 12$) at +40 mV, depolarization to +100 mV produced substantial relief from block, to 62 ± 5% of the value at −100 mV. To compare relief from block for different polyamines, we calculated the conductance ratio for responses at +50 and +100 mV. The value of $(G_{+100}/G_{+50}) - 1$ obtained for PhTX 343 (0·06 ± 0·39; $n = 5$) was not significantly different from zero, indicating no detectable relief from

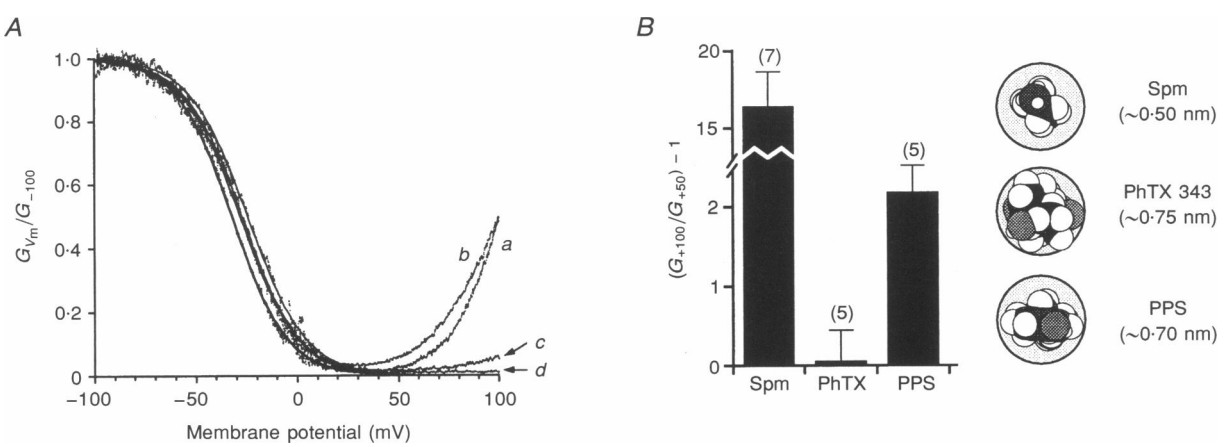

Figure 2. Relief from block by internal polyamines varies with molecular size

A, conductance–voltage plots for block by internal spermine (*a*), spermidine (*b*), PPS (*c*) and PhTX 343 (*d*) used at the same concentrations as indicated in Fig. 1. Note the smaller conductance increase at positive membrane potentials for PPS and PhTX 343 compared with spermine and spermidine. Data from individual patches were normalized to the conductance at −100 mV and pooled. Continuous lines represent fits of the Woodhull equation (infinite barrier model) over the range −100 to +20 mV. *B*, relative conductance increase on depolarization from +50 to +100 mV during block by internal spermine (Spm), PhTX 343 and PPS; error bars represent S.E.M. CPK models of the respective polyamines viewed along their narrowest axis were used to estimate minimal width and are superimposed on circles representing a pore size of diameter 0·75 nm as estimated by Burnashev *et al.* (1996).

block on depolarization from +50 to +100 mV (Fig. 2*B*). In contrast, values for PPS (2·19 ± 0·34, $n = 5$) and spermine (16·43 ± 0·45, $n = 7$) indicate substantial relief from block for these compounds.

The CPK space filling models shown in Fig. 2*B* provide a molecular correlation between experimentally observed relief from block and the size of polyamines. Along its narrowest axis, spermine is much smaller in cross-sectional width (0·44 nm) than the GluR6(Q) pore size diameter of 0·75 nm estimated by Burnashev *et al.* (1996) and in an extended conformation would be expected to permeate relatively easily, in accordance with the observed large conductance increase at positive membrane potentials. However, PhTX 343 has about the same dimensions as the pore, and would be expected to collide with amino acid residues lining the channel pore, interfering with permeation; the absence of any detectable increase in conductance between +50 and +100 mV is in agreement with this assumption. PPS takes an intermediate position between these extremes. Its diameter (0·7 nm) is slightly smaller than the permeation pathway consistent with a 2-fold increase in conductance on depolarization from +50 to +100 mV, reflecting poor but measurable permeation.

Relief from block by internal spermine varies with $[Na^+]_i$

Based on the assumption that internal spermine acts as an open channel blocker, we studied the interaction of spermine with ion flux as has been done recently for Kir channels (Lopatin & Nichols, 1996). For this purpose the reversal potential (V_{rev}) was shifted by varying first the internal and then the external concentration of the main permeant ion, Na^+. To correlate changes in permeant ion concentration with polyamine block, we compared the shift in V_{rev} with changes in the membrane potential required for half-block ($V_{½}$) by 30 μM internal spermine estimated from Boltzmann analysis.

The rectification which occurs when the Na^+ concentration differs on one side of the membrane from the other was

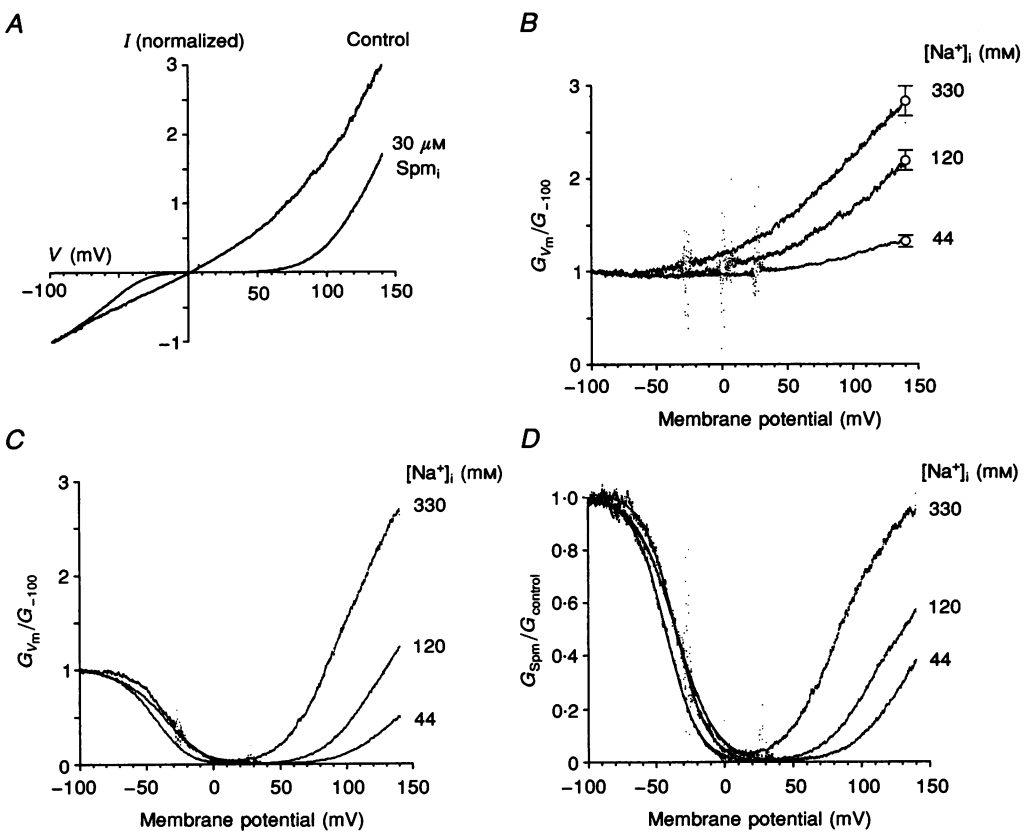

Figure 3. Increasing $[Na^+]_i$ enhances relief from block by internal spermine

A, ramp *I–V* relationships for responses to domoate in symmetrical 120 mM Na^+ (1·6 V s^{-1}); traces show pooled data with either 10 mM internal ATP (Control, $n = 6$) or 30 μM internal spermine ($n = 6$). *B*, *G–V* relationships normalized to values at −100 mV for control responses to domoate with 44 ($n = 4$), 120 ($n = 6$) or 330 mM Na_i^+ ($n = 6$) and 120 mM Na_o^+; data points around the reversal potential were masked during subsequent analysis; open symbols indicate means ± S.E.M. for responses at +140 mV for the three conditions tested. *C*, *G–V* plots for 44 ($n = 4$), 120 ($n = 6$) or 330 mM Na_i^+ ($n = 3$) with 30 μM internal spermine and 120 mM Na_o^+. *D*, *G–V* relationships for block by 30 μM internal spermine corrected for control rectification by dividing the responses shown in *C* by those shown in *B*; continuous lines represent fits of a Boltzmann function to the data between −100 and +20 mV.

expected to distort the biphasic I–V relationship resulting from polyamine block. To correct for this, control responses to domoate, with the desired Na^+ gradients, were recorded with 10 mM ATP included in the patch pipette in order to chelate residual endogenous polyamines (see Methods). Such responses were then used to evaluate block recorded in the presence of spermine using identical Na^+ gradients. I–V relationships for GluR6(Q) responses recorded with symmetrical 120 mM Na^+ during voltage ramps over the membrane potential range −100 to +140 mV had a reversal potential of $-0{\cdot}2 \pm 0{\cdot}5$ mV ($n = 6$) and showed moderate outward rectification (Fig. 3A); there was no abrupt change in slope at +40 mV as was found previously when ATP was not used to chelate residual endogenous polyamines (Bowie & Mayer, 1995). Figure 3B shows G–V plots derived from experiments with different $[Na^+]_i$. When $[Na^+]_i$ was raised to 330 mM, V_{rev} shifted to $-27{\cdot}9 \pm 0{\cdot}6$ mV ($n = 4$) and outward rectification ($G_{+140}/G_{-100} = 2{\cdot}84 \pm 0{\cdot}23$) was stronger than with symmetrical 120 mM Na^+ ($2{\cdot}20 \pm 0{\cdot}14$; $P < 0{\cdot}05$). Lowering $[Na^+]_i$ to 44 mM resulted in a positive shift in V_{rev} to $+25{\cdot}0 \pm 0{\cdot}7$ mV ($n = 4$) and there was less outward rectification ($G_{+140}/G_{-100} = 1{\cdot}33 \pm 0{\cdot}09$; $P < 0{\cdot}01$).

When similar experiments were performed with 30 μM internal spermine, the I–V relationship for GluR6(Q) responses showed pronounced biphasic rectification (Fig. 3A). Although the rectification properties were drastically changed by internal spermine, the shift in V_{rev} which occurred on increasing $[Na^+]_i$ to 330 mM ($-28{\cdot}5 \pm 0{\cdot}5$ mV; $n = 3$) or lowering $[Na^+]_i$ to 44 mM ($+26{\cdot}4 \pm 0{\cdot}7$ mV; $n = 4$) was similar to the shift recorded in control experiments. G–V plots for block by internal spermine with different $[Na^+]_i$ are shown in Fig. 3C and reveal components of rectification reflecting both polyamine block and the result of asymmetric $[Na^+]$ gradients. To analyse block by internal spermine, independent of rectification due to asymmetric $[Na^+]$ gradients, normalized G–V plots were generated by dividing the G–V plots recorded with polyamines (Fig. 3C) by the appropriate controls recorded with polyamine-free internal solution. Fits of a Boltzman function to the resulting G–V plots over the range −100 to +20 mV revealed little change in the voltage dependence of block by internal spermine when $[Na^+]_i$ was varied over the range 44–330 mM (Fig. 3D). The $V_{½}$ values for block by 30 μM internal spermine were $-40{\cdot}4 \pm 1{\cdot}6$ mV for symmetrical 120 mM Na^+ ($n = 15$), $-35{\cdot}5 \pm 0{\cdot}2$ mV for 330 mM Na_i^+ ($n = 3$) and $-38{\cdot}6 \pm 0{\cdot}5$ for 44 mM Na_i^+ ($n = 4$). The slope factors for an e-fold change in conductance were also similar: $14{\cdot}8 \pm 0{\cdot}7$ mV for symmetrical 120 mM Na^+; $12{\cdot}2 \pm 0{\cdot}2$ mV for 330 mM Na_i^+; and $15{\cdot}2 \pm 0{\cdot}8$ mV for 44 mM Na_i^+. Despite the similar voltage dependence for onset of block by spermine in these experiments, the corrected G–V plots in Fig. 3D show that relief from block by internal spermine was strongly dependent on $[Na^+]_i$. At a membrane potential of +140 mV, with 330 mM Na_i^+, relief from block reached $94{\cdot}9 \pm 1{\cdot}4$%, much greater than for 120 mM Na_i^+ ($56{\cdot}8 \pm 3{\cdot}0$%) and 44 mM Na_i^+ ($37{\cdot}7 \pm 2{\cdot}1$%).

Voltage dependence of block by internal spermine varies with $[Na^+]_o$

To examine the effect of a change in $[Na^+]_o$ on internal spermine block, voltage ramps over the range −150 to +100 mV were applied in low (44 mM), symmetrical (120 mM) and high (330 mM) external Na^+. As would be expected, inward currents evoked by domoate were either smaller (44 mM external Na^+) or larger (330 mM external Na^+) than with symmetrical 120 mM Na^+ and showed biphasic rectification with 30 μM internal spermine (Fig. 4A); the decrease in domoate-activated conductance on lowering $[Na^+]_o$ was larger than expected on the basis of constant field rectification, possibly reflecting a requirement of extracellular Na^+ for agonist binding or activation of channel gating by agonist, comparable to effects observed previously for NMDA receptors (Ozawa, Iino & Tsuzuki, 1990; Ruppersberg, von Kitzing & Schoepfer, 1994). Similar to results obtained with different $[Na^+]_i$, the shift in V_{rev} due to a change in $[Na^+]_o$ was not altered by polyamine block. In the presence of 30 μM internal spermine, lowering $[Na^+]_o$ to 44 mM shifted V_{rev} to $-28{\cdot}7 \pm 0{\cdot}9$ mV ($n = 7$) and increasing $[Na^+]_o$ to 330 mM induced a positive shift in V_{rev} to $+30{\cdot}2 \pm 3{\cdot}0$ ($n = 4$); in the absence of polyamines V_{rev} shifted to $-30{\cdot}0 \pm 1{\cdot}1$ mV with 44 mM Na_o^+ ($n = 5$), and to $+29{\cdot}9 \pm 2{\cdot}0$ mV with 330 mM Na_o^+ ($n = 8$).

Control responses recorded with internal ATP added to chelate endogenous polyamines were used to correct for rectification due to changes in $[Na^+]_o$ as described above. The resulting analysis revealed a strong shift in the voltage dependence for block by internal spermine as $[Na^+]_o$ was increased from 44 to 330 mM (Fig. 4B). Boltzmann functions fitted to corrected G–V plots over the range −100 to +20 mV for 120 mM Na_o^+, with appropriate adjustments of the fitted range for other $[Na^+]_o$, yielded $V_{½}$ values for block by 30 μM internal spermine of $-69{\cdot}0 \pm 0{\cdot}8$ mV ($n = 7$) for 44 mM Na_o^+; $-40{\cdot}4 \pm 1{\cdot}6$ mV for symmetrical 120 mM Na^+; and $-3{\cdot}9 \pm 1{\cdot}9$ mV ($n = 4$) for 330 mM Na_o^+. However, despite the large shifts in $V_{½}$ the slope factors of the Boltzmann functions for spermine block with 44 mM external Na^+ ($16{\cdot}9 \pm 1{\cdot}8$ mV, $n = 7$) and 330 mM external Na^+ ($15{\cdot}0 \pm 0{\cdot}3$ mV, $n = 4$) were similar to the value obtained with symmetrical 120 mM Na^+ ($14{\cdot}8 \pm 0{\cdot}7$ mV) and comparable to results obtained when $[Na^+]_i$ was varied. The strong coupling between shifts in $V_{½}$ for block by 30 μM internal spermine and shifts in V_{rev} due to changes in $[Na^+]_o$ but not $[Na^+]_i$ is illustrated in Fig. 5A. Also shown is the strong influence of $[Na^+]_i$ on relief from block by internal spermine at +140 mV. The strong correlation between $[Na^+]_o$ but not $[Na^+]_i$ and the voltage dependence of internal spermine block are similar to the behaviour of Kir channels which occurs when $[K^+]_o$ but not $[K^+]_i$ is varied (Lopatin & Nichols, 1996). The major difference seems to be the pronounced relief from polyamine block at positive membrane potentials which occurs only in glutamate receptor channels.

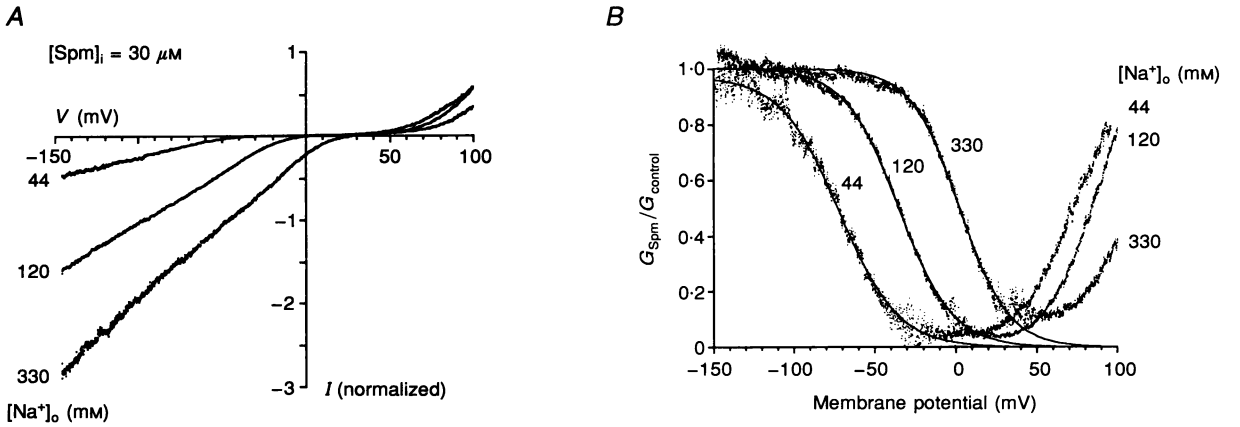

Figure 4. Increasing $[Na^+]_o$ lowers affinity for block by internal spermine

A, ramp *I–V* relationships for responses to domoate recorded with 330, 120 and 44 mM Na_o^+, 120 mM Na_i^+, and 30 μM internal spermine (1·6 V s^{-1}). Traces show pooled data normalized to responses at −100 mV with symmetrical 120 mM Na^+ and were obtained from 4 patches tested with both 120 and 330 mM Na_o^+ and 7 patches tested with both 120 and 44 mM Na_o^+. *B*, *G–V* relationships for block by 30 μM internal spermine fitted by Boltzmann functions; correction for rectification of control responses was performed as described in Fig. 3. Note the parallel shift in *G–V* plots for block by spermine with no change in the steepness of block when $[Na^+]_o$ was varied from 44 to 330 mM.

Polyamines as sole charge carriers for GluR6(Q) channels

The strong interaction of $[Na^+]_o$ with block by internal spermine could occur if spermine acts as an open channel blocker which is knocked out of the pore by Na^+ ions entering from the external solution. Furthermore, the correlation between the molecular size of polyamine analogues and the observed relief from block at positive membrane potentials (Fig. 2) supports the idea that spermine and spermidine can pass through the channel. However, the sensitivity to $[Na^+]_i$ of the relief from block by internal spermine (Fig. 3) suggests that the large outward currents at strongly positive membrane potentials illustrated in Figs 3 and 4 is most likely to result from Na^+ flux rather than currents carried by polyamines themselves. In order to demonstrate unambiguously that polyamines can indeed permeate through the pore of GluR6(Q) channels, we performed experiments in which different polyamines were used as the sole external charge carrier. Permeability values relative to Na^+ were then calculated from the reversal potentials for bi-ionic solutions. The limiting factor in these experiments is the requirement that the permeation rate for

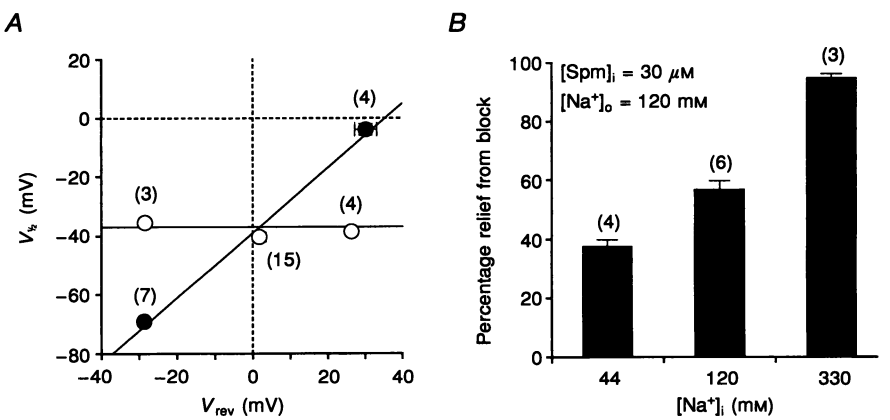

Figure 5. Coupling between E_{Na} and block by internal spermine

A, correlation between $V_{½}$ for block by 30 μM internal spermine and shifts in V_{rev} evoked by changes in $[Na^+]_o$ (●) but not $[Na^+]_i$ (○); data points show means ± S.E.M. from experiments illustrated in Figs 3 and 4. Continuous line represents a linear fit for changes in $[Na^+]_o$ (slope, 1·10; $r = 0·996$); for changes in $[Na^+]_i$ the slope (−0·06, $r = 0·67$) was not significantly different from zero; dotted lines indicate 0 mV. *B*, relief from block by 30 μM internal spermine when $[Na^+]_i$ was varied from 44 to 330 mM with $[Na^+]_o$ constant at 120 mM; correction for control rectification was performed as described in Fig. 3. Values show means ± S.E.M. of conductance ratios at +140/−100 mV for 44 ($n = 4$), 120 ($n = 6$) and 330 mM Na_i^+ ($n = 3$).

polyamines be high enough to generate measurable inward currents. For these experiments all of the external Na^+ was replaced by putrescine, spermidine or spermine (90 mM) and residual endogenous polyamines in the internal solution were chelated by the inclusion of ATP in the patch pipette.

Figure 6*A* shows current–voltage plots for GluR6(Q) responses to domoate recorded using ramp hyperpolarizations from +100 to −120 mV, with 150 mM internal Na^+ and either NMG or polyamines as sole external charge carriers. With 150 mM external NMG, currents reversed sign at $-83{\cdot}6 \pm 1{\cdot}5$ mV ($n = 7$). Calculation of relative permeabilities gave $P_{NMG}/P_{Na} = 0{\cdot}04 \pm 0{\cdot}002$, slightly higher than the value of 0·01 for P_{NMG}/P_{Cs} obtained by Burnashev *et al.* (1996). Similar to NMG, polyamines carried small inward currents indicating that they acted as permeant ions; indeed, at −120 mV currents for 90 mM putrescine (reversal potential, $-12{\cdot}4 \pm 0{\cdot}6$ mV; $n = 7$) were on average $8{\cdot}2 \pm 0{\cdot}2$ times larger than those for 150 mM NMG. For the other polyamines tested, only the currents carried by spermidine were large enough to determine reliably the reversal potential ($-32{\cdot}7 \pm 1{\cdot}4$ mV, $n = 6$) in all patches studied. The calculated permeability ratios were $P_{Put}/P_{Na} = 0{\cdot}42 \pm 0{\cdot}01$ and $P_{Spd}/P_{Na} = 0{\cdot}07 \pm 0{\cdot}005$. For spermine, we obtained reversal potentials of −42 and −47 mV in two out of five patches with large enough currents for analysis ($P_{Spm}/P_{Na} = 0{\cdot}02$). The low permeability of spermidine and spermine required accurate measurement of leak currents for estimation of reversal potentials; for 90 mM spermidine the slope resistance measured from −40 to −80 mV in the absence of agonist was 172 ± 29 GΩ with a $2{\cdot}3 \pm 0{\cdot}3$-fold increase in conductance in the presence of domoate ($n = 6$); for two patches with measurable responses to spermine the mean slope resistance in the absence of agonist was 135 GΩ with a 1·5-fold increase in conductance in the presence of domoate ($n = 2$); for putrescine, currents were large enough that accurate measurements were easily obtained (Fig. 6). However, despite the relatively high permeability for putrescine calculated from reversal potential measurements, current amplitudes at negative membrane potentials were small compared with those carried by Na^+, and at positive membrane potentials there was pronounced block of outward Na^+ current when either putrescine, spermidine, spermine or NMG were used as sole charge carriers (Fig. 6*B*). Obviously, GluR6(Q) channels are blocked by polyamines and by NMG. This is likely to be because these ions bind to GluR6(Q) channels with higher affinity than Na^+.

Block of GluR6(Q) channels by external spermine

To characterize better the block of GluR6(Q) channels by external spermine, independent of the action of cytoplasmic polyamines which would interfere with such analysis if performed using whole-cell recording, we performed concentration jump experiments in which spermine was applied to outside-out patches at doses between 3 μM and 3 mM, with equal Na^+ concentrations (150 mM) on either side of the membrane. ATP was added to the internal solution to chelate both endogenous polyamines and spermine which was expected to pass through the pore. Block by spermine was rapid in onset and weakly voltage dependent (Fig. 7*A*). At −40 mV there was 91 ± 1% block by 3 mM spermine ($n = 19$), the highest concentration applied, whereas at +80 mV, the most depolarized potential examined, the same concentration caused only 72 ± 3% block ($n = 4$). Complete block of GluR6(Q) responses was not observed at any of the membrane potentials tested. Fits of a

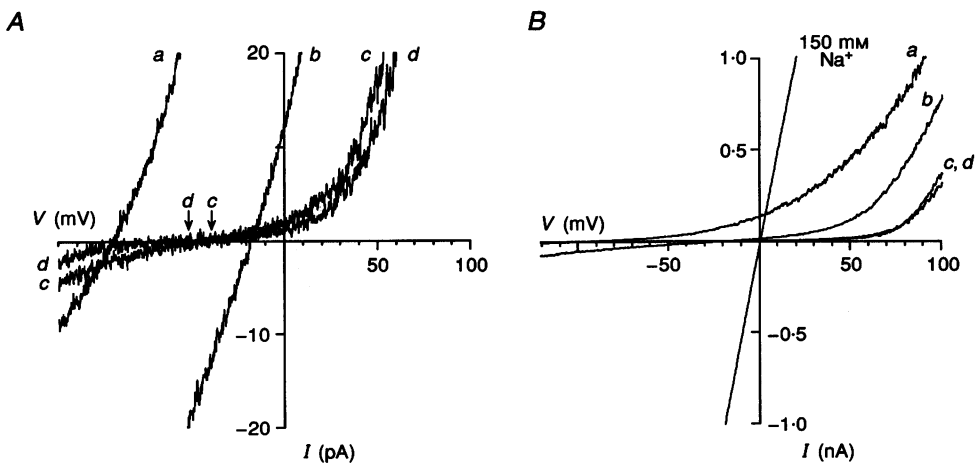

Figure 6. Polyamine permeability of GluR6(Q)

A, ramp *I–V* relationships (0·4 V s^{-1}) recorded in the same patch for GluR6(Q) responses to domoate with 150 mM NMG (*a*), 90 mM putrescine (*b*), 90 mM spermidine (*c*) or 90 mM spermine (*d*) as sole external charge carriers; leak subtraction was performed using responses recorded with the appropriate cations but without agonist. Arrows indicate reversal potentials for spermine (−42 mV) and spermidine (−32 mV). *B*, when plotted on a 50-fold lower gain the same responses reveal strong block of outward Na^+ flux by polyamines. The response for 150 mM symmetrical Na^+ was recorded in another patch also tested with NMG and scaled appropriately.

modified logistic equation accounting for the observed incompleteness of block, which is likely to reflect in part a low rate of permeation of spermine, resulted in an apparent K_d value of 167 μM at +80 mV with an increase in affinity at +40 mV (K_d, 54 μM), as expected for voltage-dependent open channel block by an external cation. However, the K_d values at +40 and −40 mV were about equal (54 and 52 μM, respectively) and at −80 mV the K_d value increased to 78 μM (Fig. 7*B*). Apparently, the block by external spermine was dependent on the membrane potential in a complex fashion that could not be described by a first order relationship.

To compare the voltage dependence for block by external and internal spermine over the same membrane potential range we plotted values for K_d as a function of membrane potential. Values for external block were obtained as shown in Fig. 7*B*; values for internal block were published previously (Bowie & Mayer, 1995). The K_d for block by internal spermine decreased e-fold per 20 mV depolarization ($z\theta = 1{\cdot}29$) over the range −80 to +40 mV (Fig. 7*C*). For external spermine block, however, the voltage dependence of K_d followed a biphasic relationship best described by the sum of two exponential functions with opposite and unequal voltage dependence (Fig. 7*C*): an e-fold decrease per 52 mV depolarization ($z\delta = 0{\cdot}49$), and an e-fold increase per 36 mV depolarization ($z\delta = 0{\cdot}72$).

Woodhull analysis of block by spermine

To study the voltage dependence for block by external spermine over a wider range of membrane potential than could be easily approached with equilibrium dose–response analysis, voltage ramp protocols similar to those in Fig. 2 were used to analyse block by 30 μM external spermine (Fig. 8*A*). These experiments were performed with a spermine-free internal solution containing 10 mM Na_2ATP. To reduce the possibility for block from the cytoplasmic face of the membrane, by spermine which had passed through the ion channel pore when the driving force was strongly negative, the membrane potential was ramped from +140 to −100 mV, and 10 mM internal Na_2ATP was used to chelate residual spermine in the bulk intracellular solution; when

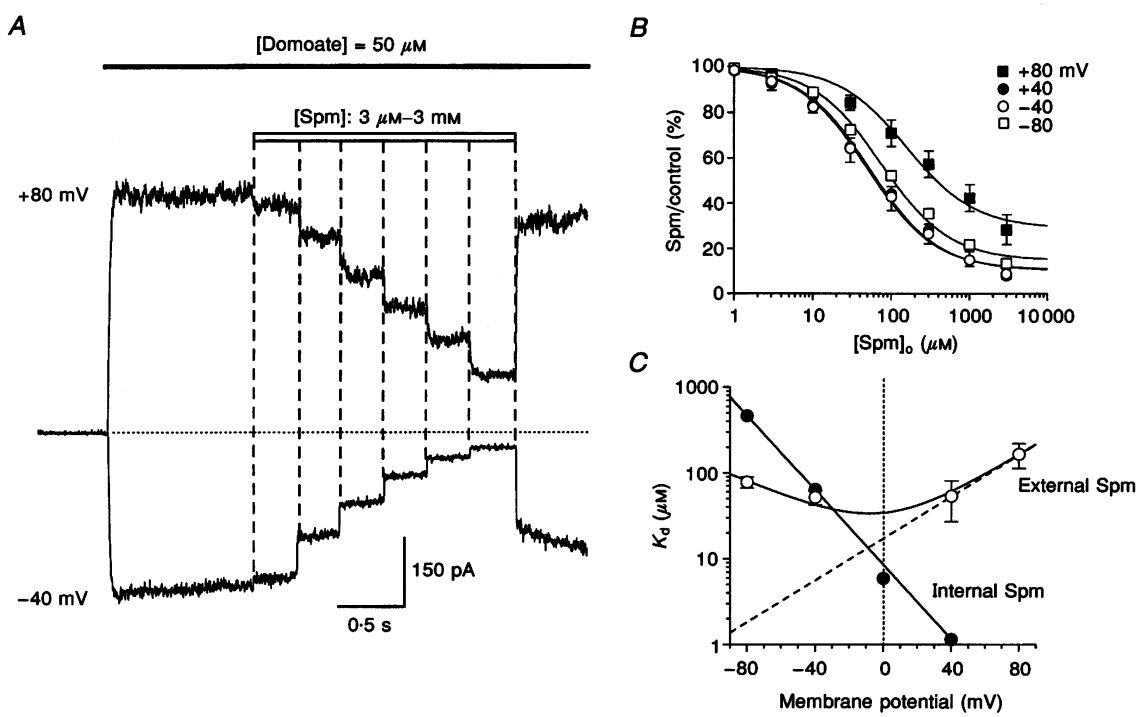

Figure 7. Block by external spermine shows weak voltage dependence

A, concentration jump responses at −40 and +80 mV to application of 3 μM to 3 mM spermine (open bar) applied in the presence of 50 μM domoate (filled bar) with symmetrical 150 mM Na^+; step increases in spermine concentration are indicated by vertical dashed lines. Full recovery from block following removal of spermine was obtained but is incomplete on the time scale shown. *B*, dose–inhibition plots for block by external spermine at −80 ($n = 9$), −40 ($n = 19$), +40 ($n = 17$) and +80 mV ($n = 4$); data points show means ± S.D. Continuous lines show fits of a logistic equation modified to account for incomplete block at saturating concentrations of spermine. *C*, voltage dependence of K_d values for dose–inhibition analysis of block by external and internal spermine (values for internal spermine are from Bowie & Mayer, 1995); error bars show S.E.M. The K_d for block by internal spermine is well fitted by an e-fold decrease per 20 mV depolarization. The biphasic change in K_d for block by external spermine is fitted by the sum of two exponential functions with opposite voltage dependence (e-fold decrease per 36 mV hyperpolarization, indicated by the dashed line, and e-fold increase per 52 mV hyperpolarization). The vertical dotted line indicates 0 mV.

these precautions were not taken there was a substantial transient block during depolarization from −100 to +140 mV, possibly caused by spermine molecules which have exited the pore and accumulated in or close to the internal vestibule of the pore.

Values for steady state block by 30 μM external spermine at −80, −40, +40 and +80 mV obtained from experiments shown in Fig. 7 superimposed well on the normalized conductance trace obtained from voltage ramp analysis (Fig. 8*A*) indicating that block was at equilibrium. Fitting the Woodhull infinite barrier model of ion channel block over the membrane potential range +20 to +140 mV gave a $K_{d(0)}$ of 37·8 ± 6·4 μM and a $z\delta$ value of 0·55 ± 0·03 ($n = 5$) for block by 30 μM external spermine. The $K_{d(0)}$ value of 38 μM for external spermine block obtained from this voltage ramp experiment is in excellent agreement with the K_d estimate of 34 μM derived from equilibrium dose–inhibition analysis at fixed membrane potentials (Fig. 7*C*). However, over the membrane potential range 0 to −100 mV, the conductance recorded in the presence of 30 μM external spermine was much larger than predicted by an infinite barrier model suggesting that block by external spermine is relieved with hyperpolarization. To accommodate this we analysed block by spermine using the approach developed by Woodhull (1973) to describe the action of permeable blockers.

The Woodhull model for a permeable blocker fitted reasonably well the biphasic voltage dependence for onset and relief from block by external spermine over the range −100 to +140 mV, such that data points for equilibrium block by spermine now superimposed on the predicted *G–V* relationship at both hyperpolarized and depolarized membrane potentials (Fig. 8*A*). A similar analysis also gave good fits for block by 30 μM internal spermine, fully accounting for relief of block with strong depolarization (Fig. 8*B*). However, the rate constants and $z\delta$ values required to fit block by external ($z\delta = 0{\cdot}56$) and internal ($z\delta = 4{\cdot}66$) spermine differed considerably, and values which fitted well data for block by external spermine predicted much weaker relief from block for internal spermine than observed experimentally and vice versa (Fig. 8). Fits of the Woodhull permeable blocker model to data for 30 μM external spermine predicted that once bound, spermine was 1·5 times more likely to pass through the channel than to return to the outside solution at 0 mV membrane potential; however, fits to block by 30 μM internal spermine predicted that once bound, spermine was 13·8 times more likely to return to the inside than to pass through the channel at 0 mV. With solutions containing 30 μM spermine on both sides of the membrane it was impossible to fit accurately the experimentally observed *G–V* relationships with the Woodhull model for a permeable blocker.

DISCUSSION

Common functional properties of GluR and Kir channels

Our results reveal a number of similarities between the block by internal polyamines of GluR channels and the classical properties of 'anomalous' rectification originally described for potassium channels (Katz, 1949; Hagiwara, Miyazaki & Rosenthal, 1976; Hagiwara & Yoshii, 1979), including a strong voltage dependence of rectification and coupling of gating to changes in the external concentration of the main permeant ion. For recombinant Kir2.1 estimates for the voltage sensitivity of intrinsic gating, an e-fold decrease in conductance per 12–18 mV depolarization

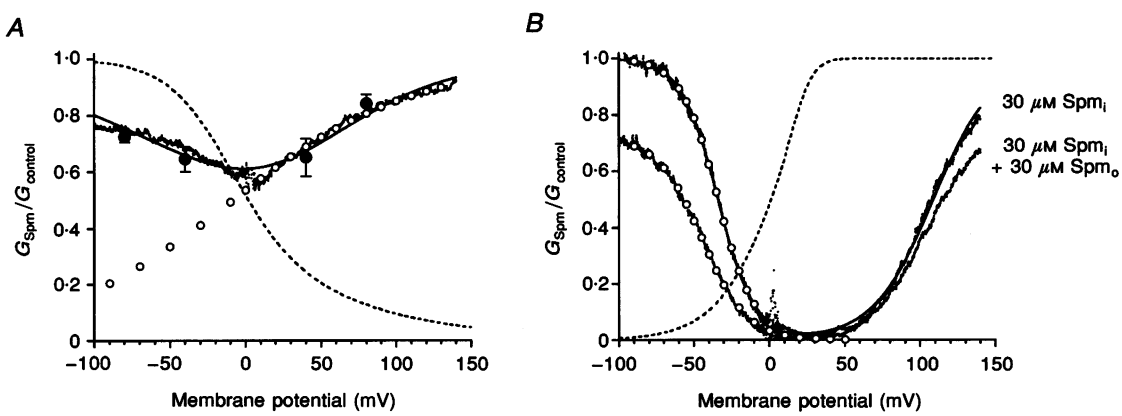

Figure 8. Voltage dependence of block by external and internal spermine

A, pooled data for block by 30 μM external spermine ($n = 5$) recorded with voltage ramps from +140 to −100 mV (1·6 V s^{-1}); responses were corrected for control rectification as described in Fig. 3. ●, data (means ± S.E.M.) from Fig. 7*B* for equilibrium block by 30 μM external spermine at −80, −40, +40 and +80 mV. ○, fits for a Woodhull infinite barrier model. *B*, similar plots recorded with voltage ramps from −100 to +140 mV (1·6 V s^{-1}) for block by 30 μM internal spermine both in the absence (Spm$_i$, $n = 5$) and presence (Spm$_i$ + Spm$_o$, $n = 4$) of 30 μM external spermine. ○, fits for a Woodhull infinite barrier model. Continuous lines in *A* and *B* represent fits of the Woodhull equation for a permeable blocker; dashed lines indicate the response predicted for 30 μM spermine applied internally (*A*) or externally (*B*).

(Stanfield *et al.* 1994*a*; Fakler *et al.* 1995) are similar to those for Kir2.1 block by experimentally applied spermine and spermidine, an e-fold decrease per 10–12 mV depolarization (Lopatin *et al.* 1994; Yang, Jan & Jan, 1995). The similar kinetics and voltage dependence of polyamine block and intrinsic gating lead to the hypothesis that channel block by polyamines underlies the intrinsic gating of Kir channels, although an allosteric effect of polyamines on an intrinsic gating mechanism remains a possible alternative mechanism (Aleksandrov, Velimirovic & Clapham, 1996). The voltage dependence for block by spermine of GluR6, e-fold decrease per 13–20 mV, is only slightly weaker than that for Kir2.1, and similar to the restoration of inward rectification for Kir channels by polyamines; experimentally applied spermine and spermidine produce biphasic *I–V*s for GluRs comparable to responses recorded in intact cells.

Similar to results for Kir2.1 (Lopatin & Nichols, 1996), we found a parallel shift in $V_{½}$ and V_{rev} for GluR block by spermine when $[Na^+]_o$ but not $[Na^+]_i$ was varied. Lopatin, Makhina & Nichols (1996) explained their findings with a model in which K^+ ions bind with high affinity to an externally located site which cannot be reached by internal polyamines. Occupancy by K^+ ions of the external binding site leads to electrostatic interaction with other cations in the pore including polyamines. The resulting destabilization of spermine binding by external K^+ underlies the coupling between E_K and $V_{½}$ when $[K^+]_o$ but not $[K^+]_i$ is altered. Such a model would need modification to describe the behaviour of GluR channels since we show that polyamines can pass through the pore. However, similarities in the dependence of polyamine block on external but not internal permeant ion concentrations for both GluR and Kir channels raises the possibility of a common molecular mechanism for block, perhaps due to structural similarities in the pore regions.

Recent work suggests that the pore of GluR channels is formed by a loop structure analogous to that in potassium channels, but with an inverted orientation (Wo & Oswald, 1995; MacKinnon, 1995; Kuner, Wollmuth, Karlin, Seeburg & Sakmann, 1996). Point mutation of single residues within the membrane domains of both GluR and Kir channels strongly interferes with rectification: in GluR channels, exchanging glutamine (Q) for arginine (R) at the Q/R-site abolishes biphasic rectification and polyamine block (Verdoorn *et al.* 1991; Bowie & Mayer, 1995). In Kir channels a single residue in the M2 domain, asparagine (Kir1.1), aspartate (Kir2.1), or glutamate (Kir4.1), is similarly important for the strength of inward rectification (Fakler *et al.* 1994; Lu & MacKinnon, 1994; Stanfield *et al.* 1994*b*; Wible, Taglialatela, Ficker & Brown, 1994; Yang *et al.* 1995). However, the gating mechanism appears to be more complex than for GluRs, since in Kir2.1 a residue located in the C-terminal domain independently controls rectification (Yang *et al.* 1995). Another difference between GluR and Kir channels is that Kir channel gating is controlled by both polyamines and Mg^{2+}, with competition between these ions for binding within Kir channels (Stanfield *et al.* 1994*a*; Fakler *et al.* 1995; Yamashita, Horio, Yamada, Takahashi, Kondo & Kurachi, 1996). In contrast, we did not observe any interaction of Mg^{2+} ions with internal polyamine block, in agreement with the previous finding that inclusion of Mg^{2+} in a polyamine-free internal solution did not restore biphasic rectification in GluR channels (Bowie & Mayer, 1995; Donevan & Rogawski, 1995).

Permeation of polyamines through GluR channels

Probably the most striking difference between GluR and Kir channels is the development of large outward currents at positive membrane potentials which is observed only for GluR channels. Our finding that this relief from internal polyamine block is inversely correlated to the size of the blocker molecule provides direct experimental support for the proposal that the blocking particle itself can permeate (Bowie & Mayer, 1995; Koh *et al.* 1995; Burnashev *et al.* 1996). Such a mechanism has a precedent from work on squid axon potassium channels which show relief from internal Na^+ block at extremely positive membrane potentials, but no relief from block for the much larger cation tetraethylammonium (French & Wells, 1977). Permeation of polyamines through GluR but not Kir channels seems a reasonable hypothesis given the much smaller diameter of the selectivity filter for potassium channels. Pore size estimates suggest cross-sectional areas of 0·442 nm^2 for GluR6 (Burnashev *et al.* 1996), but only 0·086 nm^2 for potassium channels (Hille, 1973), far too small to allow passage of a polyamine molecule (cross-sectional area 0·16 nm^2). For GluR6(Q) the largest inward currents with polyamines as sole external charge carriers were obtained with putrescine, consistent with flux inversely correlated to affinity for binding to the pore, since putrescine has the lowest affinity of the endogenous polyamines for block of GluR6 (Bowie & Mayer, 1995).

GluR block by external spermine

It has been shown recently that externally applied spermine can block AMPA-type glutamate receptors (Washburn & Dingledine, 1996); this was confirmed in the present series of experiments for kainate receptor channels. For GluR6(Q), external spermine block is much weaker than internal spermine block and its voltage dependence very shallow; at very negative membrane potentials we observed pronounced relief from block resulting from permeation of the blocker. However, relief from internal and external spermine block strongly differ in their voltage dependence, such that polyamine permeation seems to occur much more easily from the outside than from the inside. Further evidence for this was obtained from analysis using the Woodhull model for a permeable blocker (Fig. 8), which indicated that at 0 mV, spermine was 20 times more likely to pass through the channel when applied from the outside than when

spermine entered the channel from the internal mouth. Although we have yet to obtain kinetic data which address the underlying mechanism of this asymmetry, experiments with changes in $[Na^+]_i$ and $[Na^+]_o$ reveal strong interactions between the main permeant ion and polyamines. Thus, raising $[Na^+]_i$ promotes relief from internal block at potentials positive to V_{rev} probably by increasing the permeation of polyamines, while raising $[Na^+]_o$ destabilizes spermine binding, probably reflecting ion–ion interactions within the pore or outer vestibule of the channel.

An Eyring rate theory model for GluR6(Q)

The model of ion channel block developed by Woodhull (1973) describes the behaviour of molecules like spermine which can pass through the pore of a channel, and thus reach their binding site from either side of the membrane. However, the most widely used versions of Woodhull's equations are the special cases for which either the external or internal barrier is infinitely high, preventing the blocker from passing through the pore; although simple to use, these equations are inappropriate for polyamine block of GluRs since they do not describe the relief from block which underlies the biphasic *I–V* relations recorded with internal spermine. Woodhull's equations for a permeant blocker make the assumptions that the major permeant ion does not compete with blocker for its binding site, and that the current carried by the blocker is negligible compared with that carried by the main permeant ion. Although these assumptions are probably reasonable approximations for many channels, the first is clearly violated in the case of GluR block by polyamines.

An alternative approach to the description of channel block is the use of rate theory models based on principles developed by Eyring (Woodbury, 1971). The simplest version of such a model has two barriers and one binding site (2b1s) and is equivalent to the case modelled by Woodhull with the extensions that competition between the permeant ion and blocker are allowed, and current carried by the blocker itself can be predicted. Attempts to develop a 2b1s model which accounted for the biphasic voltage dependence of block by both external and internal spermine failed because the barrier and well profiles required to generate biphasic *I–V* relations with stronger block by internal than external spermine predicted much higher permeability for spermine than measured with bi-ionic solutions. A model with one additional binding site and barrier (3b2s), when fitted to our data for block by 30 μM internal and 30 μM external spermine, successfully predicted both biphasic *G–V* plots and the low permeability of spermine in bi-ionic solutions (Fig. 9). Barrier–well values (outside to inside) for Na^+ (10·81, −2·07, 10·08, −2·08 and 7·87*RT*) were chosen to give a conductance of 21 pS based on estimates for the main conductance state of GluR6(Q) (Swanson, Feldmeyer, Kaneda & Cull-Candy, 1996); values for spermine were 14·27, −3·50, 0, −13·96 and 11·80*RT*; electrical distances (δ) between adjacent barriers and wells were 0·08, 0·152, 0·17, 0·082, 0·405 and 0·111; the barriers were asymmetrical to increase the steepness of the voltage dependence of onset and relief from block by spermine. The model also included electrostatic repulsion between ions when both sites were occupied as described by Davies *et al.* (1996); the repulsion factors were $r_{Na-Na} = 3{\cdot}0$, $r_{Na-Spm} = 7{\cdot}0$, $r_{Spm-Spm} = 20$. Fits of a Woodhull infinite barrier model for block by 30 μM internal spermine over the range −100 to +20 mV gave $z\theta = 1{\cdot}7$ and $K_{d(0)} = 2{\cdot}4$ μM, similar to experimentally recorded values. In bi-ionic solutions, with 150 mM Na_o^+ and 90 mM Spm_i the reversal potential was −26 mV ($P_{Spm}/P_{Na} = 0{\cdot}06$). Although, the model predicted increased relief from block when $[Na^+]_i$ was increased from 44 to 330 mM, it failed to predict accurately the strong

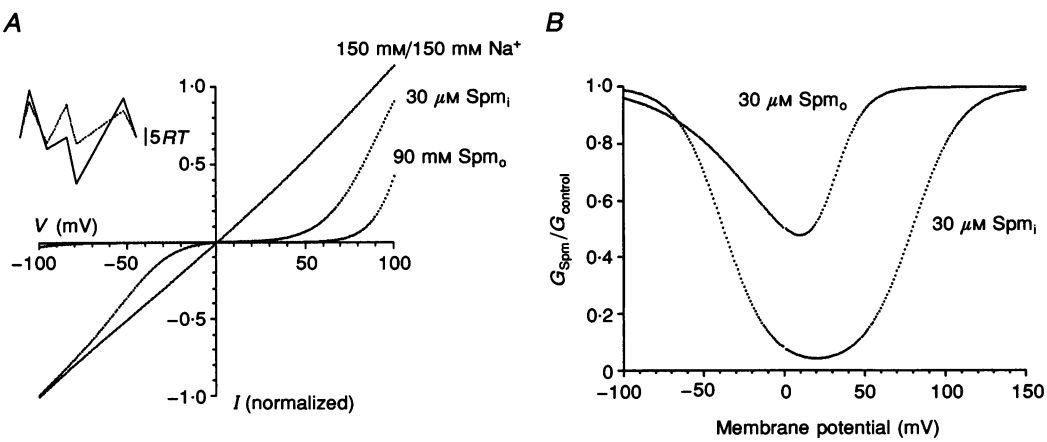

Figure 9. Eyring rate theory model for permeation and block by spermine

A, *I–V* relationships for a 3b2s model with symmetrical 150 mM Na^+ for the same solution with 30 μM internal spermine, and for a bi-ionic solution with 90 mM external spermine and 150 mM internal Na^+. The inset shows the barrier well profile for Na^+ (continuous line) and spermine (dotted line). *B*, conductance–voltage plots generated by the same model for block of responses with 150 mM symmetrical Na^+ by 30 μM external (Spm_o) and 30 μM internal (Spm_i) spermine.

coupling between $[Na^+]_o$ and block by internal spermine. At present we have not been able to overcome this limitation using a 3b2s model, and since there is no experimental evidence suggesting that GluR channels behave as long pores with more than two ion binding sites we did not investigate more complex models.

Polyamine binding sites in GluR channels

The molecular identity and location of the polyamine binding site(s) within GluR channels are not known with certainty. RNA editing at the Q/R site (Verdoorn *et al.* 1991) is likely to disrupt polyamine block in GluR6(R) due to charge repulsion between a ring of positively charged arginines in the pore and the ionized amine groups in spermine. It has yet to be confirmed that in AMPA and kainate receptors, a conserved negative charge (Glu or Asp) four residues downstream of the Q/R site represents a site which interacts strongly with polyamines (Dingledine, Hume & Heinemann, 1992) and it is unknown whether there are additional residues involved in channel block. Assuming a single site, fits of the Woodhull infinite barrier model to block by internal and external spermine gave $z\theta$ and $z\delta$ values of 1·97 and 0·55, respectively; because $\theta = 1 - \delta$ this gives $\theta = 0{\cdot}78$, and a valence of 2·52 for block by spermine, indicating that the binding site is deep in the electric field with respect to the internal face, and that not all of the charges on spermine contribute to binding. The similar $z\delta$ values for block by spermine ($z = +4$) and by spermidine, PPS or PhTX 343 (all $z = +3$) support the latter conclusion. However, the rate theory model which better describes polyamine block contains two binding sites ($\theta = 0{\cdot}516$ and 0·768) with the higher affinity site located only 50% through the electric field.

In the rate theory models currently used to analyse channel block, ions are modelled as point charges; the extended structure of spermine, in which the terminal amine groups are separated by 1·6 nm, suggests that this is inappropriate. Thus, for any site which interacts strongly with spermine, it is probable that each of the amines will sequentially interact with this site as spermine passes through the pore; any structure based model would then need to address the coupled movement of four ionized residues within the electric field. To address these issues, the residues which interact with polyamines as they pass through the pore need to be identified, and new theories for ion channel block will be required to account for the action of molecules with distributed charges. The importance of accurately modelling channel block is well illustrated by current controversy as to whether polyamine-induced rectification of potassium channels occurs via an allosteric mechanism or open channel block (Aleksandrov *et al.* 1996). Allosteric modulation and open channel block are not mutually exclusive and can occur simultaneously, for example in the case of NMDA receptor block by Mg^{2+} (Li-Smerin & Johnson, 1996).

Aleksandrov, A., Velimirovic, B. & Clapham, D. E. (1996). Inward rectification of the IRK1 K^+ channel reconstituted in lipid bilayers. *Biophysical Journal* **70**, 2680–2687.

Begenisich, T. B. & Cahalan, M. D. (1980). Sodium channel permeation in squid axons. I: Reversal potential experiments. *Journal of Physiology* **307**, 217–242.

Bowie, D. & Mayer, M. L. (1995). Inward rectification of both AMPA and kainate subtype glutamate receptors generated by polyamine-mediated ion channel block. *Neuron* **15**, 453–462.

Brooks, S. P. & Storey, K. B. (1992). Bound and determined: A computer program for making buffers of defined ion concentrations. *Analytical Biochemistry* **201**, 119–126.

Burnashev, N., Villarroel, A. & Sakmann, B. (1996). Dimensions and ion selectivity of recombinant AMPA and kainate receptor channels and their dependence on Q/R site residues. *Journal of Physiology* **496**, 165–173.

Colquhoun, D. & Hawkes, A. G. (1987). A note on correlations in single ion channel records. *Proceedings of the Royal Society* B **230**, 15–52.

Davies, N. W., McKillen, H. C., Stanfield, P. R. & Standen, N. B. (1996). A rate theory model for Mg^{2+} block of ATP-dependent potassium channels of rat skeletal muscle. *Journal of Physiology* **490**, 817–826.

Dingledine, R., Hume, R. I. & Heinemann, S. F. (1992). Structural determinants of barium permeation and rectification in non-NMDA glutamate receptor channels. *Journal of Neuroscience* **12**, 4080–4087.

Donevan, S. D. & Rogawski, M. A. (1995). Intracellular polyamines mediate inward rectification of Ca^{2+}-permeable α-amino-3-hydroxy-5-methyl-4-isoxazolepropionic acid receptors. *Proceedings of the National Academy of Sciences of the USA* **92**, 9298–9302.

Doupnik, C. A., Davidson, N. & Lester, H. A. (1995). The inward rectifier potassium channel family. *Current Opinion in Neurobiology* **5**, 268–277.

Fakler, B., Brändle, U., Bond, C., Glowatzki, E., Konig, C., Adelman, J. P., Zenner, H. P. & Ruppersberg, J. P. (1994). A structural determinant of differential sensitivity of cloned inward rectifier K^+ channels to intracellular spermine. *FEBS Letters* **356**, 199–203.

Fakler, B., Brändle, U., Glowatzki, E., Weidemann, S., Zenner, H. P. & Ruppersberg, J. P. (1995). Strong voltage-dependent inward rectification of inward rectifier K^+ channels is caused by intracellular spermine. *Cell* **80**, 149–154.

Ficker, E., Taglialatela, M., Wible, B. A., Henley, C. M. & Brown, A. M. (1994). Spermine and spermidine as gating molecules for inward rectifier K^+ channels. *Science* **266**, 1068–1072.

French, R. J. & Wells, J. B. (1977). Sodium ions as blocking agents and charge carriers in the potassium channel of the squid giant axon. *Journal of General Physiology* **70**, 707–724.

Hagiwara, S., Miyazaki, S. & Rosenthal, N. P. (1976). Potassium current and the effect of cesium on this current during anomalous rectification of the egg cell membrane of a starfish. *Journal of General Physiology* **67**, 621–638.

Hagiwara, S. & Yoshii, M. (1979). Effects of internal potassium and sodium on the anomalous rectification of the starfish egg as examined by internal perfusion. *Journal of Physiology* **292**, 251–265.

Hille, B. (1973). Potassium channels in myelinated nerve. Selective permeability to small cations. *Journal of General Physiology* **61**, 669–686.

Hille, B. (1992). *Ionic Channels of Excitable Membranes.* Sinauer Associates, Sunderland, MA, USA.

Isa, T., Iino, M., Itazawa, S. & Ozawa, S. (1995). Spermine mediates inward rectification of Ca^{2+}-permeable AMPA receptor channels. *NeuroReport* **6**, 2045–2048.

Kamboj, S. K., Swanson, G. T. & Cull-Candy, S. G. (1995). Intracellular spermine confers rectification on rat calcium-permeable AMPA and kainate receptors. *Journal of Physiology* **486**, 297–303.

Katz, B. (1949). Les constantes électriques de la membrane du muscle. *Archives des Sciences Physiologiques* **2**, 285–299.

Koh, D. S., Burnashev, N. & Jonas, P. (1995). Block of native Ca^{2+}-permeable AMPA receptors in rat brain by intracellular polyamines generates double rectification. *Journal of Physiology* **486**, 305–312.

Kuner, T., Wollmuth, L. P., Karlin, A., Seeburg, P. H. & Sakmann, B. (1996). Structure of the NMDA receptor channel M2 segment inferred from the accessibility of substituted cysteines. *Neuron* **17**, 343–352.

Li-Smerin, Y. & Johnson, J. W. (1996). Effects of intracellular Mg^{2+} on channel gating and steady-state responses of the NMDA receptor in cultured rat neurons. *Journal of Physiology* **491**, 137–150.

Lopatin, A. N., Makhina, E. N. & Nichols, C. G. (1994). Potassium channel block by cytoplasmic polyamines as the mechanism of intrinsic rectification. *Nature* **372**, 366–369.

Lopatin, A. N., Makhina, E. N. & Nichols, C. G. (1996). A simple barrier model is sufficient to explain 'crossover' effect and correct shift of inward rectification induced by multivalent polyamines. *Biophysical Journal* **70**, A301.

Lopatin, A. N. & Nichols, C. G. (1996). $[K^+]$ dependence of polyamine-induced rectification in inward rectifier potassium channels (IRK1, Kir2.1). *Journal of General Physiology* **108**, 105–113.

Lu, Z. & MacKinnon, R. (1994). Electrostatic tuning of Mg^{2+} affinity in an inward-rectifier K^+ channel. *Nature* **371**, 243–246.

MacKinnon, R. (1995). Pore loops: an emerging theme in ion channel structure. *Neuron* **14**, 889–892.

Neher, E. (1992). Correction for liquid junction potentials in patch clamp experiments. *Methods in Enzymology* **207**, 123–131.

Ozawa, S., Iino, M. & Tsuzuki, K. (1990). Suppression by extracellular K^+ of *N*-methyl-D-aspartate responses in cultured rat hippocampal neurons. *Journal of Neurophysiology* **64**, 1361–1367.

Palmer, B. N. & Powell, H. K. J. (1974). Complex formation between 4,9-diazododecane-1,12-diamine (spermine) and copper(II) ions and protons in aqueous solution. *Journal of the Chemical Society Dalton Transactions* **19**, 2086–2088.

Press, W. H., Teukolsky, S. A., Vetterling, W. T. & Flannery, B. P. (1992). *Numerical Recipes in Fortran. The Art of Scientific Computing.* Cambridge University Press, Cambridge, UK.

Ruppersberg, J. P., von Kitzing, E. & Schoepfer, R. (1994). The mechanism of magnesium block of NMDA receptors. *Seminars in the Neurosciences* **6**, 87–96.

Stanfield, P. R., Davies, N. W., Shelton, P. A., Khan, I. A., Brammar, W. J., Standen, N. B. & Conley, E. C. (1994*a*). The intrinsic gating of inward rectifier K^+ channels expressed from the murine IRK1 gene depends on voltage, K^+ and Mg^{2+}. *Journal of Physiology* **475**, 1–7.

Stanfield, P. R., Davies, N. W., Shelton, P. A., Sutcliffe, M. J., Khan, I. A., Brammar, W. J. & Conley, E. C. (1994*b*). A single aspartate residue is involved in both intrinsic gating and blockage by Mg^{2+} of the inward rectifier, IRK1. *Journal of Physiology* **478**, 1–6.

Swanson, G. T., Feldmeyer, D., Kaneda, M. & Cull-Candy, S. G. (1996). Effect of RNA editing and subunit co-assembly on single-channel properties of recombinant kainate receptors. *Journal of Physiology* **492**, 129–142.

Verdoorn, T. A., Burnashev, N., Monyer, H., Seeburg, P. H. & Sakmann, B. (1991). Structural determinants of ion flow through recombinant glutamate receptor channels. *Science* **252**, 1715–1718.

Vyklicky, L., Benveniste, M. & Mayer, M. L. (1990). Modulation of *N*-methyl-D-aspartic acid receptor desensitization by glycine in mouse cultured hippocampal neurones. *Journal of Physiology* **428**, 313–331.

Washburn, M. S. & Dingledine, R. (1996). Block of alpha-amino-3-hydroxy-5-methyl-4-isoxazolepropionic acid (AMPA) receptors by polyamines and polyamine toxins. *Journal of Pharmacology and Experimental Therapeutics* **278**, 669–678.

Wible, B. A., Taglialatela, M., Ficker, E. & Brown, A. M. (1994). Gating of inwardly rectifying K^+ channels localized to a single negatively charged residue. *Nature* **371**, 246–249.

Wo, Z. G. & Oswald, R. E. (1995). Unravelling the modular design of glutamate-gated ion channels. *Trends in Neurosciences* **18**, 161–168.

Woodbury, J. W. (1971). Eyring rate theory model of the current–voltage relationships of ion channels in excitable membranes. In *Chemical Dynamics: Papers in Honor of Henry Eyring*, ed. Hirschfelder, J. O. & Henderson, D., pp. 601–617. John Wiley & Sons Inc., New York.

Woodhull, A. M. (1973). Ionic blockage of sodium channels in nerve. *Journal of General Physiology* **61**, 687–708.

Yamashita, T., Horio, Y., Yamada, M., Takahashi, N., Kondo, C. & Kurachi, Y. (1996). Competition between Mg^{2+} and spermine for a cloned IRK2 channel expressed in a human cell line. *Journal of Physiology* **493**, 143–156.

Yang, J., Jan, Y. N. & Jan, L. Y. (1995). Control of rectification and permeation by residues in two distinct domains in an inward rectifier K^+ channel. *Neuron* **14**, 1047–1054.

Acknowledgements

We thank Dr P. Seeburg for the gift of plasmids, Professor K. Nakanishi for PhTX 343, and Dr C. J. McBain for comments on the manuscript.

Author's email address

M. L. Mayer: mlm@helix.nih.gov

Received 10 March 1997; accepted 2 May 1997.